

Functional oxide layers for electrical isolation and chemical passivation of steel substrates

Johann Dorn

July 18, 2021

Abstract

A thin zirconium oxide layer was aufgetragen via doctor blading on a steel foil substrate with the goal of erhalten an moeglichst homogenous and insulating layer. The layers were characterized over the current-voltage curve and the operational variables were optimized with an pso swarm optimization algorithm.

Preface

Nam dui ligula, fringilla a, euismod sodales, sollicitudin vel, wisi. Morbi auctor lorem non justo. Nam lacus libero, pretium at, lobortis vitae, ultricies et, tellus. Donec aliquet, tortor sed accumsan bibendum, erat ligula aliquet magna, vitae ornare odio metus a mi. Morbi ac orci et nisl hendrerit mollis. Suspendisse ut massa. Cras nec ante. Pellentesque a nulla. Cum sociis natoque penatibus et magnis dis parturient montes, nascetur ridiculus mus. Aliquam tincidunt urna. Nulla ullamcorper vestibulum turpis. Pellentesque cursus luctus mauris.

Contents

1	Introduction	5
2	Aims and Objectives	5
3	Theoretical Background aka How does it work?	5
3.1	Sputtering	5
3.2	SEM	5
3.3	Infrared absorbance	5
3.4	Particle Swarm Optimization	5
3.5	Machine Learning	5
4	Experimental	5
4.1	Substrate Preparation	5
4.2	Solutions	6
4.2.1	Aquatic solution	6
4.2.2	Buthanolic solution	6
4.3	Doctor blading	7
4.4	Calcination	8
4.5	Characterisation	9
4.6	Finding base process	9
5	Evaluation and Computational Details	9
5.1	Evaluation of Samples	9
5.2	Sample Selection	10
5.3	EMMA Propagation	11
5.4	Fitting via Machine Learning	11
6	Results and Discussion	13
6.1	XRD	13
7	Outlook	13

Acronyms

1F one-fold concentrated solution. 6

2F two-fold concentrated solution. 6, 7

3F three-fold concentrated solution. 7

4F four-fold concentrated solution. 7

5F five-fold concentrated solution. 7

AcOH acetic acid. 7

BuOH 1-buthanol. 6, 7, 13

CIGS copper indium gallium sulfide. 5

DB doctor blading. 7

FTO fluorine doped tin oxide. 5

H₂O deionized water. 5, 6

H₂SO₄ sulfuric acid. 6

Hacac acetylacetone. 6, 7, 13

HCl hydrochloric acid. 6

IPO 2-Propanol. 6, 7

ITO indium doped tin oxide. 5

N₂ nitrogen. 6

NaOH sodium hydroxide. 6

PV photovoltaic. 5

SDS sodium dodecyl sulfate. 6

SG sol-gel. 5

Zr(PrO)₄ zirconium(IV)propoxide. 6, 7, 13

ZrO₂ zirconium dioxide. 5

1 Introduction

describe everything what is mentioned in 4 Photovoltaic (PV) is one big hope when trying to become carbon neutral as it uses the energy provided by sun directly in contrast to renewable energy sources (e.g. wind and water) or even carbon based sources. One sort of PV are copper indium gallium sulfide (CIGS) [1] cells. In order to make a module, multiple cells are operated in series. The cells must be applied to a non-conducting surface. Glass is a good non-conducting substrate, but very rigid and brittle. An alternative is steel, which is ductile, inexpensive and highly available, but conducting. An insulating layer must therefore be applied to the steel substrate before any CIGS cells can be applied. A non-toxic material which is suitable for this application is zirconium dioxide (ZrO_2). An economic and scalable method is doctor blading via a sol-gel (SG) process. SG processes often produce porous layers. In this work a dense, insulating and homogeneous layer is pursued. ML can help to uncover complex non-linear relations, such as the influence of the production factors on the thickness and resistance of the resulting layer. The minimisation of the conductance if performed with a particle swarm optimization algorithm.

2 Aims and Objectives

The aim of this work is to develop a non-conducting layer on steel based on non-toxic materials like Aluminium or Zirconium via doctor blading. This layer can then be used as insulator for CIGS modules on steel sheets. Doctor blading - or tape casting - is a widely used precision coating method to apply thin films on large area surfaces[2]. This sol-gel process was chosen because of the availability to the industrial partner. In order to optimize the resulting layer the multitude of parameters was optimized with an particle swarm optimization ansatz. The conductivity (dependent variable), the number of layers and calcination time (both independent variables) should be minimized.

3 Theoretical Background aka How does is work?

3.1 Sputtering

3.2 SEM

3.3 Infrared absorbance

3.4 Particle Swarm Optimization

3.5 Machine Learning

4 Experimental

In this section the used chemicals and substrates, experimental procedures and any used equipment are described.

4.1 Substrate Preparation

Five different substrates were used throughout this work: microscope glass slides ($2.5\text{ cm} \times 7.5\text{ cm}$) from **Sigma Aldrich**, thinner, squared glass plates ($2.5\text{ cm} \times 2.5\text{ cm}$) from **Sigma Aldrich**, indium doped tin oxide (ITO) glass plates ($2.5\text{ cm} \times 2.5\text{ cm}$) from **Sigma Aldrich**, fluorine doped tin oxide (FTO) glass plates ($5\text{ cm} \times 5\text{ cm}$) from **Sigma Aldrich** and steel foil ($10\text{ cm} \times 10\text{ cm}$) provided by Sunplugged GmbH (<http://sunplugged.at/>). The glass slides and FTO were scratched with a scratching tool and broken with a **glass breaker** into pieces with dimensions $2.5\text{ cm} \times 2.5\text{ cm}$. The steel foil was cut with a foil cutter, a cutter knife (repeatedly), a paper cutter or a scissors (ordered by increasing curvature of resulting plates). All substrates were cleaned in three steps before usage:

1. 15 min in 50 mL deionized water (H_2O) and 1 mL of Hellmanex III in a sonic bath

2. 15 min in H₂O in a sonic bath
3. 15 min in 2-Propanol (IPO) in a sonic bath

After the last cleaning step, the samples were blown dry with dry nitrogen (N₂) gas.

4.2 Solutions

Two main recipes were used and their compositions were varied. The first recipe - adopted from Anwar et. al. [3] - was based on zirconium(IV)propoxide (Zr(PrO)₄) in acetylacetone (Hacac) and H₂O. The second recipe - adopted from Hu et. al. [4] - was based on Zr(PrO)₄ in 1-butanol (BuOH).



(a) Aquatic solution



(b) Buthanolic solution

Figure 1: Aquatic and buthanolic solution in beaker glass with magnetic stirring bars sealed with Parafilm

4.2.1 Aquatic solution

Zr(PrO)₄ was added to Hacac while stirring and in a separate vessel H₂O (including any optional additives such as sodium dodecyl sulfate (SDS), hydrochloric acid (HCl), sulfuric acid (H₂SO₄) or sodium hydroxide (NaOH)) was added to IPO and both were stirred for one hour. The H₂O-IPO mixture was added to the other solution and stirred over night. The exact volumes can be taken from table 1.

Table 1: Compositions of different aquatic solutions

recipe	1	2	3	4	5	6	7
Zr(PrO) ₄ [mL]	8	8	8	8	8	8	8
Hacac [mL]	8	8	8	8	8	8	8
IPO [mL]	2	2	2	2	2	2	2
H ₂ O [mL]	2.6	2.6	2.5	2	2	2	2
SDS [mg]	-	5.9	-	-	-	-	-
HCl [mL]	-	-	-	-	0.5	-	-
H ₂ SO ₄ [mL]	-	-	-	-	-	0.5	-
NaOH [mL]	-	-	-	-	-	-	0.5

4.2.2 Buthanolic solution

Five different concentration were prepared. The one-fold concentrated solution (1F) was closest to the recipe proposed by Hu et. al. [4]. The other four solutions (two-fold concentrated solution (2F),

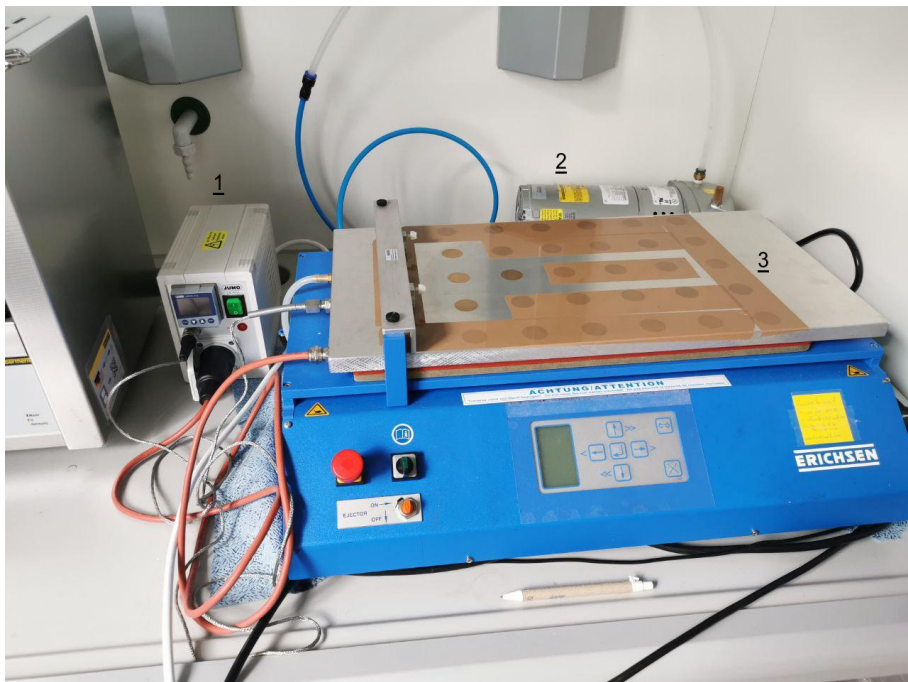


Figure 2: (1) Temperature regulator on the left, (2) vacuum pump in the background and (3) Erichsen Coatmaster 510 with heatable vacuum plate. The majority of the suction areas is sealed with tape to increase the under pressure at the remaining ones. **add picture with blade**

three-fold concentrated solution (3F), four-fold concentrated solution (4F), five-fold concentrated solution (5F)) were similar with higher concentrations of $\text{Zr}(\text{PrO})_4$ (see table 2).

Table 2

	1F	2F	3F	4F	5F
BuOH [mL]	4.95	4.9	4.85	4.8	4.75
$\text{Zr}(\text{PrO})_4$ [mL]	0.05	0.1	0.15	0.2	0.25
Hacac [mL]	0.0125	0.025	0.0375	0.05	0.0625
IPO/acetic acid (AcOH) [mL]	2	2	2	2	2

The solvent (BuOH) was put into a beaker glass (or similar, preferably with an air-tight cap) with a stirrer and $\text{Zr}(\text{PrO})_4$ was added while stirring. After stirring 15 min one mole equivalent chelating agent (Hacac) was added and stirred for another 15 min. Finally, the stabilisation solvent[4] (IPO or AcOH) was added to the mixture and stirred for additional 30 min. In order to make a 2F solution, the volume of $\text{Zr}(\text{PrO})_4$ and Hacac was doubled and BuOH was decreased by the volume of $\text{Zr}(\text{PrO})_4$.

4.3 Doctor blading

After setting the heating plate temperature, the vacuum plate temperature (see figure 2) and the doctor blading (DB) velocity, the DB blade is put into position and the sample placed on the vacuum plate. The vacuum is switched on and the blade is sent over the sample without liquid to see if it is held in position. 100 μL of solution is applied with an 10-1000 μL pipette and the blade moves over the sample distributing the liquid evenly. After evaporation of the solution, the vacuum is turned off, the 'blade pusher' put into initial position, the blade removed and excess solution removed with a wipe. The small metal plate is transferred to the hot heating plate and rests on there for 3-5 min. The process is repeated as wished.

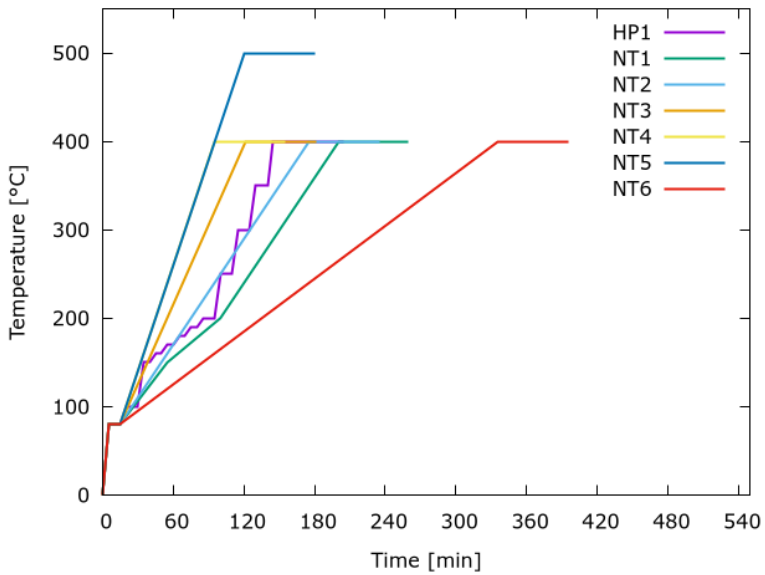


Figure 3: Different heatings curves

4.4 Calcination

A LabTech EH45 C heating plate and a Naberterm L B410 furnace were used to calcinate the doctor bladed samples. The heating late can hold temperature for a certain amount of time, but heated with a fixed rate of circa 10 °C/min. In order to achieve a lower overall heating rate several temperature ramps and plateaus were alternated (see table 3). This procedure will be called HP1 from now on, which stands for heating plate procedure. The HP1 procedure was optimized for the available hardware by a colleague working on the project prior to the author.

HP1												
T [°C]	80	100	150	160	170	180	190	200	250	300	350	400
t [min]	10	10	5	5	5	5	5	10	10	10	10	60

Table 3: Time the temperature was held constant at certain temperatures on the heating plate

The NT1 heating program was used to mimic the HP1 heating procedure in the Naberterm furnace. NT2 is an simplification of NT1 and programs NT3-NT6 are the same as NT2 with altered heating rate and partly increased calcination temperature T_{Cal} (NT5). NT2-NT6 had only 2 variables (heating rate and calcination temperature) instead of 4 (three different heating rates and calcination temperature). All heating programs were held at the calcination temperature for one hour. In figure 3 the different heating curves are depicted.

Name	80-150°C [°C/min]	150-200°C [°C/min]	200°C-T _{Cal} [°C/min]	T _{Cal} [°C]	t _{Cal} [min]
NT1	2	1	2	400	60
NT2	2	2	2	400	60
NT3	3	3	3	400	60
NT4	4	4	4	400	60
NT5	4	4	4	500	60
NT6	1	1	1	400	60

Table 4: Heating rates and calcination temperature holding times.

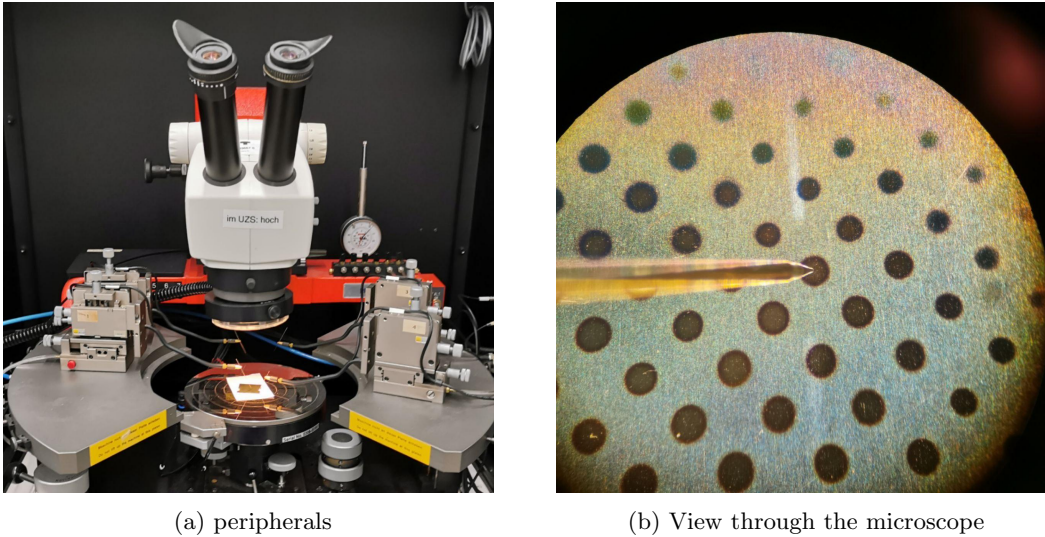


Figure 4: I-V curve abnehm aperature and sicht durch das micro scope.

4.5 Characterisation

All scanning electron microscopy images were taken with a Zeiss Supra 40. Infrared spectra were recorded with a Bruker Vertex 70 spectrometer. Diffraction spectra were obtained with a Thermo Scientific ARL Equinox 100 X-Ray Diffractometer. All spectra were taken at 5° incident angle and compared to an internal database. <https://doi.org/10.1016/B978-0-12-816806-6.00017-0> [https://chem.libretexts.org/Courses/Franklin_and_Marshall_College/Introduction_to_Materials_Characterization__CHM_412_Collaborative_Text/Diffraction_Techniques/X-ray_diffraction_\(XRD\)_basics_and_application](https://chem.libretexts.org/Courses/Franklin_and_Marshall_College/Introduction_to_Materials_Characterization__CHM_412_Collaborative_Text/Diffraction_Techniques/X-ray_diffraction_(XRD)_basics_and_application)

The current-voltage curves were measured with Agilent 4156C Precision Semiconductor Parameter Analyzer after sputtering Aluminium contacts through a mask with **Sputtering Machine** assisted by **Leybold Univex 450 C** for the vacuum.

4.6 Finding base process

After a fitting recipe was found, the process to produce an acceptable layer was untersucht. There were many variables which had to be taken into account. The damals current procedure produced clear and continuous films, but was plagued from unhomogenities due to drying stains. Using a heat gun the drying stain can be surcumvented (umgangen), but the results were unreproduceable. The glass unterlage was therefore exchanged with a metal plate which allowed both to hold the sample via underpressure and heat it to a certain temperature. The bounds fore the process were then explored. Especially the doctor blading velocity.

5 Evaluation and Computational Details

5.1 Evaluation of Samples

For every I-V curve (aluminium dot) the gradient g at $V = 0$ is calculated by taking 5 points after the origin and 5 points before the origin, averaging their V and I values and calculating i

$$g = \frac{I_{n+1} - I_n}{V_{n+1} - V_n}. \quad (1)$$

As a measure of conductance a distance D from an ideal non-conducting case. The average of the negative base 10 logarithm subtracted from an ideal non-conducting gradient of 10^{-13}

$$D = \sum_i^N \frac{-\log_{10}(g_i) - 13}{N} \quad (2)$$

Another measure is the density of shorted species ρ_s is calculated in following way:

$$s_i = \begin{cases} 1 & \text{if } -\log(g_i) < 5 \\ 0 & \text{if } -\log(g_i) \geq 5 \end{cases} \quad (3)$$

$$\rho_s = \sum_i^N \frac{s_i}{N} \quad (4)$$

Other estimates of the conductance are the averages:

$$G_1 = \log \left(\sum_i^N \frac{g_i}{N} \right) \quad (5)$$

$$G_2 = \sum_i^N \frac{\log(g_i)}{N} \quad (6)$$

5.2 Sample Selection

An evolutionary approach was chosen, namely a multi-objective Particle Swarm Optimization (PSO) with a multi-response Multivariate Adaptive Regression Splines (MARS) model[5, 6, 7, 8]. "PSO is a population based heuristic inspired by the flocking behavior of birds. To simulate the behavior of a swarm, each bird (or particle) is allowed to fly towards the optimum solution." [5] Initially the input parameters (independent variables), their boundaries and number of equidistant levels for each parameter are declared (see table 5). Next, the output variables (dependant variables), their weights in the objective function (the function which should be optimized) are specified and if they should be minimized or maximized is noted.

Zr(PrO) ₄ conc. [21 g/L]	layers	T_{DB} [°C]	v_{DB} [mm/s]	T_{cal} [°C]	v_{cal} [°C/h]
2	4	40	10	300	120
3	6	50	12	400	360
4	8	60	14	500	600
5	10	70	16		840
	12	80	18		1080
			20		

Table 5: Discrete levels of each input parameter **are concentrations correct?**

The first step is to select an initial population (ensemble of experiments), which is chosen randomly from the population space. The samples are made, measured and evaluated according to section 4 and the distance D (see eq. 2), ρ_s (see eq. 4), n_{layers} (numbers of layers) and v_{cal} (heating rate of calcination process in °C/min) are supplied to the program. The program uses this data to estimate a response for each output variable (and to choose a fraction of the initial population which is allowed to propagate). The response variables for the entire population space is calculated. The current population - each of the particles independently - moves towards the optimum solution. The population for the next time step is outputted and the experiments are again executed, measured and evaluated.

5.3 EMMA Propagation

5.4 Fitting via Machine Learning

scarce data may lead to overfitting[9]

Python and sci-kit learn **cite** was used to implement a linear fit model, and SVR with the kernels polynomial, rbf and sigmoid. The space of hyper parameters C, the degree (in case of polynomial), epsilon and gamma was scanned.

conc	layers	vDOC	TDOC	vCal	Tcal	
1	10	5	20	120	400	
1	4	0.1	20	120	500	
5	10	0.1	20	120	500	
5	4	5	20	480	400	
1	5	5	80	120	500	
1	10	1	80	480	400	
5	5	1	80	120	400	
5	10	5	80	480	500	
2	8	0.5	40	360	470	
2	6	2	40	360	430	
1	4	12	70	120	500	
1	9	18	80	240	400	
4	6	14	60	240	500	
4	6	14	60	240	500	
4	6	14	60	240	500	
2	10	20	40	120	500	6113
3	8	18	70	1080	300	2850
3	6	10	50	1080	400	5526
3	10	16	80	120	500	6554
4	6	16	80	1080	300	2947
3	12	12	80	840	500	8318
3	10	14	50	600	500	7374
5	6	10	60	1080	400	5648
5	10	20	60	360	300	3956
5	12	14	60	1080	300	2700
2	4	10	80	1080	300	6101
2	4	10	40	600	300	7201
3	4	12	60	600	300	1462
4	4	10	80	1080	300	2883
5	12	20	70	600	300	1680
2	4	10	40	120	300	1
2	4	10	40	120	500	6001
3	4	10	40	120	500	6102
5	4	10	80	1080	300	2884
5	12	20	60	120	300	360
3	4	10	40	600	400	4202
2	6	20	40	120	500	6105
5	12	14	60	600	300	1500
3	6	14	60	600	300	1486
4	4	14	80	1080	300	2923
4	8	18	80	1080	300	2971
3	8	10	50	1080	300	2530
2	12	16	40	120	400	3077
2	10	18	60	1080	300	2733
4	10	10	50	1080	300	2535

Table 6

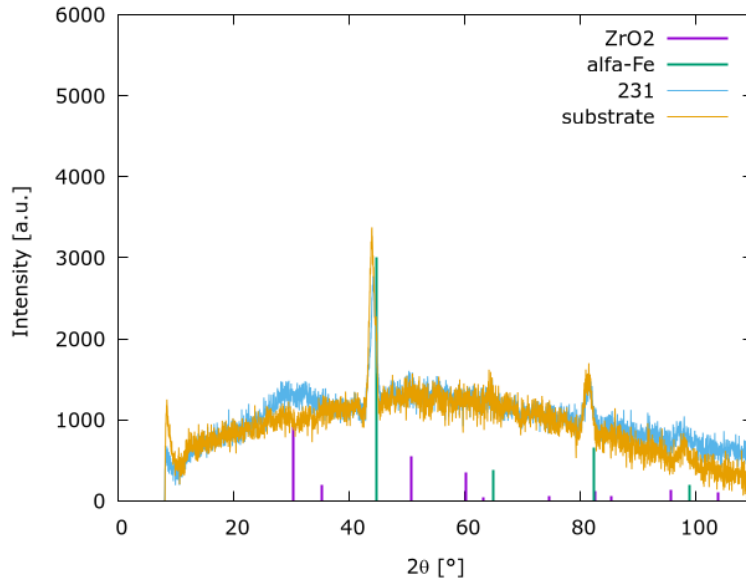


Figure 5: XRD spectra

6 Results and Discussion

Following stirring times (in minutes) were tested and didn't have an influence on stability of the solution: 10-10-20, 10-10-45, 30-30-180. The space seems to be too big for the small sample size. Look at relation of space size and sample size here and in Hu2016.

Would be easier to fit with single factor at a time variation or latin hyper cuber? Would it also be easier for PSO or ML to find fitting function? Every output var is independent of each other, so v_{cal} can act as test

plot predictions from EMMA and ML.

6.1 XRD

7 Outlook

Making of the solution for the sol-gel process: For a single concentrated solution 0.05 mL of $\text{Zr}(\text{PrO})_4$ are added while stirring to 4.95 mL of BuOH and stirred for 15 min. 0.013 mL (or one molar equivalent of Zr) of Hacac is added to the stirring solution. After another 15 min 1 mL of acetic acid is added and stirred for 30 min to stabilize the solution up to 24 h.

The concentration can be increased up to 5 times being stable for a minimum of 4 h. The sol-gel process produces am homogeneous transparent crystalline zirconia oxide layer. homogeneity can be mainly controlled via blade velocity and temperature and layers can be stacked.

It should have been alos verglichen with grid search with comparable size but most time was used to find a vernuenfig base recipe and process

It is still very human Der process is - as it the case with all ML and most fitting processes - is very abhaengig von hyper parameters, In the current work population size, number of generations, and most importantly boundaries (grenzen).

References

- [1] P. S. Vasekar, A. H. Jahagirdar, and N. G. Dhere, "Photovoltaic characterization of copper-indium-gallium sulfide (cigs2) solar cells for lower absorber thicknesses," *Thin Solid Films*, vol. 518, no. 7, pp. 1788–1790, 2010. Photovoltaics, solar energy materials and thin films - IMRC 2008, Cancun, Mexico.

- [2] A. Berni, M. Mennig, and H. Schmidt, “Doctor blade,” in *Sol-gel technologies for glass producers and users*, pp. 89–92, Springer, 2004.
- [3] M. A. Anwar, T. Kurniawan, Y. P. Asmara, W. S. W. Harun, A. N. Oumar, and A. B. D. Nandyanto, “Morphology evaluation of ZrO₂dip coating on mild steel and its corrosion performance in NaOH solution,” *IOP Conference Series: Materials Science and Engineering*, vol. 257, p. 012087, oct 2017.
- [4] B. Hu, E. Jia, B. Du, and Y. Yin, “A new sol-gel route to prepare dense al₂o₃ thin films,” *Ceramics International*, vol. 42, no. 15, pp. 16867–16871, 2016. <https://www.sciencedirect.com/science/article/pii/S0272884216312548>.
- [5] L. Villanova, P. Falcaro, D. Carta, I. Poli, R. Hyndman, and K. Smith-Miles, “Functionalization of microarray devices: Process optimization using a multiobjective pso and multiresponse mars modeling,” in *IEEE Congress on Evolutionary Computation*, pp. 1–8, IEEE, 2010.
- [6] J. Kennedy and R. Eberhart, “Particle swarm optimization,” in *Proceedings of ICNN’95-international conference on neural networks*, vol. 4, pp. 1942–1948, IEEE, 1995.
- [7] L. Breiman and J. H. Friedman, “Predicting multivariate responses in multiple linear regression,” *Journal of the Royal Statistical Society: Series B (Statistical Methodology)*, vol. 59, no. 1, pp. 3–54, 1997.
- [8] D. Carta, L. Villanova, S. Costacurta, A. Patelli, I. Poli, S. Vezzu, P. Scopece, F. Lisi, K. Smith-Miles, R. J. Hyndman, *et al.*, “Method for optimizing coating properties based on an evolutionary algorithm approach,” *Analytical chemistry*, vol. 83, no. 16, pp. 6373–6380, 2011.
- [9] Y. LeCun, Y. Bengio, *et al.*, “Convolutional networks for images, speech, and time series,” *The handbook of brain theory and neural networks*, vol. 3361, no. 10, p. 1995, 1995.